Dipole Moments of Partially Bound Lewis Acid−Base Adducts

D. L. Fiacco, Y. Mo, S. W. Hunt, M. E. Ott,† A. Roberts,‡ and K. R. Leopold*

Department of Chemistry, University of Minnesota, 207 Pleasant Street, SE, Minneapolis, Minnesota 55455

Received: September 5, 2000

Stark effect measurements have been performed on six Lewis acid−base complexes containing $^{32}SO_3$ and $^{11}BF_3$. The following dipole moments have been obtained: $HC^{14}N-SO_3$ (4.4172 ± 0.0031 D); $CH_3C^{14}N-SO_3$ (6.065 ± 0.018 D); $HC^{15}N-BF_3$ (4.1350 ± 0.0073 D); $H_3{}^{15}N-BF_3$ (5.9027 ± 0.0093 D (A state), 5.917 ± 0.010 (E state)); $(CH_3)_3{}^{15}N-BF_3$ (6.0157 ± 0.0076 D); and $(CH_3)_3{}^{15}N-B(CH_3)_3$ (4.5591 ± 0.0097 D). Across a series of complexes with a common acid, the induced dipole moment increases sharply as the dative bond shortens. Contributions to the total molecular dipole moment arising from distortion, polarization, and charge transfer have been estimated for these and a number of related complexes, using the block-localized wave function energy decomposition analysis of Mo, Gao, and Peyerimhoff. Mulliken and natural population analyses are presented, as are electron density difference maps for $HCN-SO_3$, $(CH_3)_3N-BF_3$, and $(CH_3)_3N-SO_3$. Theoretical values for the degree of charge transfer are compared with experimental estimates based on nuclear hyperfine parameters, and the validity of a simple chemical model involving charge transfer and bond moments is examined. Ab initio calculations of the induced dipole moment of $HCN-SO_3$ and H_3N-SO_3 are given as a function of N−S bond length and compared with the experimentally observed values for a series of SO_3 complexes. The results suggest that the induced moments of the series collectively approximate the induced dipole moment *function* for individual members of the series. Similar results are obtained using previously published dipole moment functions for $HCN-BF_3$ and H_3N-BF_3.

Introduction

Lewis acid−base complexes containing a partially formed dative bond offer some new and interesting perspectives on molecular structure and bonding.[1,2] Whereas the traditional definitions of van der Waals and covalent radii epitomize the sharp distinction between chemical and weak physical interactions, there is a long history of examples in the crystallographic literature[3,4] in which bond distances and bond angles lie between those characteristic of these normally recognized limits. A growing number of gas-phase and theoretical studies also indicate that molecular structure in this regime is not an immutable property of a molecule but rather exhibits an extraordinary dependence on phase.[1,2,5,6] Indeed, bond lengths and bond angles change dramatically upon crystallization, and there is significant theoretical evidence to support the idea that the molecular dipole moment function, $\mu(R)$, plays an important role in the effect.[5,7−10]

The study of Lewis acid−base complexes is, of course, not new. Recognized as early as 1923,[11] such systems have been the subject of numerous structural studies,[12] and a large volume of solution-phase data, both spectroscopic[12b,c,13] and thermodynamic,[12b−d,14] has been reported. Most closely related to the work reported here are a number of gas-phase electron diffraction[15] and microwave[16] studies that have investigated the structures of donor−acceptor complexes with fully, and in some cases partially, formed dative bonds. Matrix isolation techniques have also been applied,[17] and an increasing amount of theoretical attention has been paid to these systems in recent years.[18]

The dipole moment is an important property for donor−acceptor complexes, both in the context of phase-dependent structure, noted above, and as a fundamental measure of charge distribution. Whereas solution-phase measurements of dipole moments for acid−base complexes are certainly to be found in the literature,[12b,c,19] the values obtained are, in general, subject to the effects of solvent polarization.[12b] For gas-phase species, a number of isolated measurements now exist,[5,16a,b,d,f,g,k,20] though there appear to be few, if any, systematic investigations based on modern high-resolution techniques.

In this paper, we present Stark effect measurements for a series of six Lewis acid−base complexes in the gas phase. The dipole moments obtained are combined with literature values for several related adducts, and a number of computational methods are used to aid in the interpretation of the results. From an experimental standpoint, we examine the relationship between the dipole moment induced by complexation and the length of the donor−acceptor bond. From a theoretical perspective, we discuss not only the magnitude of the induced moments, per se, but also the relative contributions from polarization, charge transfer, and distortion. Further, in light of these theoretical results, we examine the validity of a simple chemical model of polarity based on bond moment and charge-transfer considerations. Separate calculations of the dipole moment functions, $\mu(R)$, are also presented for some of the systems studied, and their relationship with the experimentally obtained dipole moments is discussed.

Experimental Methods and Results

Spectra were recorded using a pulsed nozzle Fourier transform microwave spectrometer,[21] the details of which have been described previously.[22] The system is equipped with a pair of rectangular aluminum Stark plates, which operate in a bipolar

* To whom correspondence should be addressed.
† Present address: Western Wyoming Community College, P.O. Box 428, Rock Springs, Wyoming 82902-0428.
‡ Present address: Department of Chemistry, University of California, Berkeley, California 94720.

10.1021/jp0031810 CCC: $20.00
Published on Web 12/19/2000

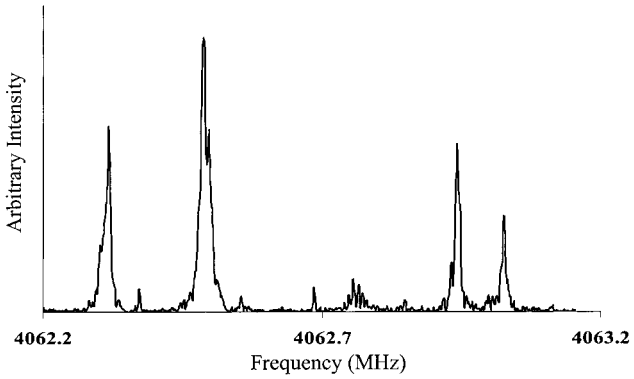

Figure 1. A portion of the $J = 2 \leftarrow 1$ and $K = \pm 1$ transition of CH_3CN-SO_3 taken at 1.55 V/cm. The four prominent components, from left to right, are the $(M_J'', M_I'') \rightarrow (M_J', M_I') = (0, -1) \rightarrow (0, -1)$ superimposed on $(0, 1) \rightarrow (1, 0)$; $(-1, 1) \rightarrow (-1, 1)$; $(0, -1) \rightarrow (0, -1)$; and $(0, 1) \rightarrow (0, 1)$. The smaller features that appear are artifacts of the microwave cavity, not molecular transitions. This spectrum represents 44 s of data-collection time.

configuration and straddle the microwave cavity to apply a uniform dc electric field to the molecular sample. For the systems studied in this work, one or more transitions previously assigned at zero electric field were examined at a series of field strengths. Little, if any, spectral broadening occurred as the electric field was increased, but the intensity of the transitions was observed to diminish. In most cases, this ultimately limited the degree to which transitions could be shifted, but the problem was not severe enough to preclude a sufficiently accurate determination of the dipole moments.

The effective plate spacing for each experiment was determined by calibration using either the $J = 1 \leftarrow 0$ transition of OCS[23] ($\mu = 0.715\,21(20)$ D) or the $J = 4 \leftarrow 3$ and $K = \pm 3$ transition $Ar-SO_3$[24] ($\mu = 0.2676(3)$ D), as described elsewhere.[20] To eliminate possible effects due to the accumulation of diffusion pump oil on the plate surfaces,[20,25] calibrated distances were obtained both before and after the collection of experimental data, and the data were admitted for analysis only upon agreement of the pre- and postcollection values.

For complexes of SO_3, which itself has no quadrupolar nuclei, measurements were made using the ordinary ^{14}N isotopic derivatives of the bases. For the $^{11}BF_3$ species, in which hyperfine structure is also present because of the boron, $^{15}NH_3$, $HC^{15}N$, and $(CH_3)_3{}^{15}N$ were used. $HC^{15}N$ was prepared by reaction of $KC^{15}N$ with dry H_3PO_4, whereas $^{15}NH_3$ was produced from $^{15}NH_4Cl$ and KOH. $(CH_3)_3{}^{15}N$ was prepared according to literature procedures.[26]

A portion of the $J = 2 \leftarrow 1$ and $K = \pm 1$ transition of CH_3CN-SO_3 taken at 1.55 V/cm is shown in Figure 1. Because the Stark shifts were not overwhelmingly large compared with the nitrogen or boron hyperfine structure, an "intermediate field" analysis was used.[20,27] The Stark Hamiltonian, $H_{Stark} = -\boldsymbol{\mu}\cdot\mathbf{E}$, was set up using a $|J,K,I,M_J,M_I,M_F\rangle$ basis in blocks diagonal in $M_F = M_J + M_I$ but off-diagonal in M_J and M_I. Matrix elements included both first- and second-order contributions to the Stark energy. Energies (and hence transition frequencies) were obtained by direct diagonalization and least-squares fitted to the experimental data. Rotational, distortion, and quadrupole coupling constants were constrained in all cases to their values determined at zero electric field, and transition frequencies were generally reproduced to within the estimated experimental uncertainties. Tables of transition frequencies, electric field strengths, and residuals from the least-squares fits are provided as Supporting Information. The results are summarized in Table 1. Values of the dipole moment, μ, the induced dipole moment, $\Delta\mu_{ind}$, and dative bond length, R, are given in Table 2, together with literature values for a number of related complexes.

Computational Methods and Results

Theoretical Background (Block-Localized Wave Function Energy Decomposition (BLW-ED) Method). Decomposition of the calculated dipole moments is based on the block-localized wave function (BLW) approach of Mo et al.[38] This approach has demonstrated much less basis set dependence with respect to polarization and charge-transfer energies than other decomposition procedures and is expected to yield reliable results for the complexes of interest here. For a monomer or dimer, the dipole moment is defined as

$$\boldsymbol{\mu} = \langle\Psi|e\mathbf{r}|\Psi\rangle \tag{1}$$

where Ψ denotes the wave function of the monomer or dimer. Generally, the dipole moment of a dimer, μ(AB), is not simply the sum of the dipole moments of two monomers (μ(A) and μ(B) for A and B, respectively), and the variation

$$\Delta\mu_{ind} = \mu(AB) - \mu(A) - \mu(B) \tag{2}$$

originates primarily from distortion, polarization, and charge-transfer effects. For weakly bound systems, vibrational averaging over large-amplitude zero-point motions can also contribute. To discriminate between the distortion, polarization, and charge-transfer components computationally, the dipole moment of the dimer at its equilibrium configuration is assumed to evolve in a successive way. First, the two monomers approach each other to form the dimer with their individual electron densities frozen (state 1). The wave function for state 1 can thus be represented as

$$\Psi^{(1)}{}_{AB} = \hat{A}(\Psi^0{}_A\,\Psi^0{}_B) \tag{3}$$

where $\Psi^0{}_A$ and $\Psi^0{}_B$ are the optimal wave functions for the distorted monomers A and B, respectively, and $\hat{A}$ is an antisymmetrizing operator. The dipole moment of state 1 is nearly equal to the sum of μ^0(A) and μ^0(B), viz.,

$$\mu^{(1)}{}_{AB} = \langle\Psi^{(1)}{}_{AB}|e\mathbf{r}|\Psi^{(1)}{}_{AB}\rangle \approx \mu^0(A) + \mu^0(B) \tag{4}$$

where μ^0(A) and μ^0(B) are the dipole moments of isolated A and B at their distorted geometries within the complex. The second equality in eq 4 is only approximate because the orbitals on A and B are assumed to be nonorthogonal, which produces cross terms in the evaluation of $\langle\Psi^{(1)}{}_{AB}|e\mathbf{r}|\Psi^{(1)}{}_{AB}\rangle$.

Next, the electron densities in A and B are allowed to relax in response to the electric field of the interacting partner (state 2). The BLW method is employed here, in which the optimal wave function in the absence of charge transfer is derived for the intermediate diabatic state. The wave function for state 2 can be written as

$$\Psi^{(2)}{}_{AB} = \hat{A}(\Psi_A\,\Psi_B) \tag{5}$$

where Ψ_A or Ψ_B is a successive product of localized molecular orbitals on monomers A and B, respectively. Whereas the orbitals on A or B are restrained to be orthogonal as in the usual molecular orbital theory, the orbitals on A are nonorthogonal to the orbitals on B. Like state 1, the dipole moment of state 2

TABLE 1: Summary of Stark Effect Measurements

molecule[a]	transitions examined	range of electric fields (V/cm)	number of transitions fitted[b]	μ (D)[c]
$HCN-SO_3$	$J = 1 \leftarrow 0, K = 0$ $J = 2 \leftarrow 1, K = 0$	15.34−73.46	41	4.4172(31)
CH_3CN-SO_3	$J = 2 \leftarrow 1, K = 0, \pm 1$	0.61−30.75	68	6.065(18)
$HC^{15}N-{}^{11}BF_3$	$J = 1 \leftarrow 0, K = 0$	12.33−36.88	44	4.1350(73)
$H_3{}^{15}N-{}^{11}BF_3$ (A state)	$J = 1 \leftarrow 0, K = 0$	6.28−43.05	34	5.9027(93)
$H_3{}^{15}N-{}^{11}BF_3$ (E state)	$J = 1 \leftarrow 0, K = 0$	6.28−43.05	32	5.917(10)
$(CH_3)_3{}^{15}N-{}^{11}BF_3$	$J = 1 \leftarrow 0, K = 0$ $J = 2 \leftarrow 1, K = 0, \pm 1$	0.47−36.89	115	6.0157(76)
$(CH_3)_3{}^{15}N-{}^{11}B(CH_3)_3$	$J = 1 \leftarrow 0, K = 0$ $J = 2 \leftarrow 1, K = 0, \pm 1$	0.42−36.82	122	4.5591(97)[d]

[a] Unless otherwise indicated, the common isotopic form was observed. [b] This number includes multiple observations of individual transitions at several different values of the applied electric field. [c] Uncertainties are 1 standard error in the least-squares fit. [d] Measured for the more intense of two observed vibrational states.

TABLE 2: Dipole Moment Data for Selected Lewis Acid−Base Complexes

species	μ (D)	ref[a]	$\Delta\mu_{ind}$ (D)[b]	R (Å)[c]	ref[d]
N_2-SO_3	0.46(1)	24	0.46	2.9[e]	
$HCN-SO_3$	4.4172(31)	*f*	1.433	2.577(6)	32
CH_3CN-SO_3	6.065(18)	*f*	2.147	2.466(16)	32
H_3N-SO_3	6.204(11)	20	4.733	1.957(23)	33
$(CH_3)_3N-SO_3$	7.1110(69)	16k	6.499	1.912(20)	16k
H_3N-SO_3[g]	9.6(6)	34	8.1	1.7714(3)	35
$HCN-BF_3$	4.1350(73)	*f*	1.150	2.473(29)	36
H_3N-BF_3	5.9027(93)	*f*	4.431	1.673(10)	16i
$(CH_3)_3N-BF_3$	6.0157(76)	*f*	5.404	1.636(4)	16c
H_3N-BH_3	5.216(17)	16f	3.745	1.6576(16)	16f
$(CH_3)_3N-BH_3$	4.84(10)	16b	4.23	1.638(10)	16b
$(CH_3)_3N-B(CH_3)_3$	4.5591(97)	*f*	3.947	1.698(10)	16e, 37

[a] Reference for dipole moment data. [b] Calculated using the following moments for the basic moiety: N_2 (0 D); HCN (2.9846(15) D, ref 28); CH_3CN (3.9185(20) D, ref 29); NH_3 (1.47149(15) D, ref 30); and $(CH_3)_3N$ (0.612 D, ref 31). [c] Dative bond length (B−N or S−N). [d] Reference for structural data. [e] Estimated from van der Waals radii. [f] This work. [g] Solid-state values.

is approximately equal to the sum of $\mu_{BLW}(A)$ and $\mu_{BLW}(B)$:

$$\mu^{(2)}{}_{AB} \equiv \mu_{BLW}(AB) = \langle \Psi^{(2)}{}_{AB} | e\mathbf{r} | \Psi^{(2)}{}_{AB} \rangle \approx \mu_{BLW}(A) + \mu_{BLW}(B) \quad (6)$$

where $\mu_{BLW}(A)$ and $\mu_{BLW}(B)$ are defined as

$$\mu_{BLW}(A) = \langle \Psi_A | e\mathbf{r} | \Psi_A \rangle \quad (7)$$

$$\mu_{BLW}(B) = \langle \Psi_B | e\mathbf{r} | \Psi_B \rangle \quad (8)$$

The difference between $\mu_{BLW}(A)$ or $\mu_{BLW}(B)$ and $\mu^0(A)$ or $\mu^0(B)$ demonstrates the effect of polarization on the individual monomers. Moreover, the energy variation between states 1 and 2 is the polarization energy.

Finally, electrons in the dimeric complex are permitted to flow freely, and we reach the final state Ψ_{AB}, where all molecular orbitals are delocalized over the entire system. The comparison between $\mu^{(2)}{}_{AB}$ and the final calculated moment, $\mu_{HF}(AB)$, yields the charge-transfer component to the dipole moment, and the energy variation between the states $\Psi^{(2)}{}_{AB}$ and Ψ_{AB} can be defined as the charge-transfer stabilization energy.

BLW Results. Calculations were performed for the systems represented in Table 2 using the BLW program and Gaussian 98.[40] The results are summarized in Tables 3−5. Table 3 gives bimolecular complex geometries optimized at the HF/6-31G-(d) level and compares them with those of the experimental data, where available. Agreement with the experiment is seen to be reasonable, with the possible exception of CH_3CN-BF_3, for which the calculated bond length is about 0.50 Å too long. Electron correlation and basis set superposition are expected to be important for this system and likely account for the discrepancy. However, BLW calculations at higher levels of theory are not, at present, possible, and thus the above level of calculation was used to maintain uniformity throughout. The HF/6-31G(d) calculations, however, are seen to reproduce the essential variations in structural parameters across the series of complexes considered and should, therefore, be adequate for making rough quantitative assessments of the terms contributing to the overall molecular dipole moments.

Results of the BLW calculations are given in Tables 4 and 5. Table 4 gives the dipole moments of the acids and bases at the distorted complex geometry, $\mu^0(X)$ (X = A or B) and in the presence of the second monomer using the BLW wave function $\mu_{BLW}(X)$. The intermediate dipole moments for the complex

TABLE 3: Structural Parameters of Lewis Acid−Base Adducts[a]

species	R_{XY} expt. (Å)	R_{XY} theor. (Å)	θ^b (donor) theor.	α^c (acceptor) expt.	α^c (acceptor) theor.
$N_2\cdots SO_3$	*d*	3.058	180.0	*d*	90.3
$HCN\cdots SO_3$	2.577(6)	2.704	180.0	91.8(4)	91.5
$CH_3CN\cdots SO_3$	2.466(16)	2.620	180.0	92.0(7)	92.0
$H_3N\cdots SO_3$	1.957(23)	1.951	109.7	97.6(4)	97.5
$(CH_3)_3N\cdots SO_3$	1.912(20)	1.898	108.7	100.1(2)	99.4
$HCN\cdots BF_3$	2.473(29)	2.601	180.0	*d*	92.4
$CH_3CN\cdots BF_3$[e]	2.011(7)	2.506	180.0	95.6(6)	93.4
$H_3N\cdots BF_3$	1.673(10)	1.693	110.6	*d*	103.6
$(CH_3)_3N\cdots BF_3$	1.636(4)	1.679	109.1	106.4(3)	105.0
$H_3N\cdots BH_3$	1.6576(16)	1.689	110.9	104.69(11)	104.3
$(CH_3)_3N\cdots BH_3$	1.638(10)	1.677	109.3	105.32(16)	105.2
$H_3N\cdots B(CH_3)_3$	*d*	1.739	111.1	*d*	103.9
$(CH_3)_3N\cdots B(CH_3)_3$	1.698(10)	1.825	110.5	108.0(15)	106.5

[a] Unless otherwise noted, experimental data are from references given in Table 2. [b] Angle formed by the acceptor atom (B or S), the nitrogen atom, and the first atom of the base bonded to nitrogen. [c] NBF or NSO angle. [d] Not determined experimentally. [e] Reference 39.

TABLE 4: Computed Dipole Moments (D) Using the BLW-ED Approach[a]

	Lewis base (B)				Lewis acid (A)			
species	μ_{EXP}(B)[b]	μ^0_{eq}(B)	μ^0(B)	μ_{BLW}(B)	μ^0(A)	μ_{BLW}(A)	μ_{BLW}(AB)	μ_{HF}(AB)
$N_2\cdots SO_3$	0.0	0.0	0.0	0.28	0.0	0.11	0.41	0.46
$HCN\cdots SO_3$	2.985	3.21	3.21	3.79	0.22	0.55	4.35	4.57
$CH_3CN\cdots SO_3$	3.919	4.04	4.03	4.83	0.30	0.71	5.55	5.87
$H_3N\cdots SO_3$	1.472	1.92	1.79	2.68	1.09	2.14	4.80	6.88
$(CH_3)_3N\cdots SO_3$	0.61	0.74	0.94	2.83	1.35	2.67	5.49	7.86
$HCN\cdots BF_3$	2.985	3.21	3.21	3.61	0.31	0.50	4.11	4.22
$CH_3CN\cdots BF_3$	3.919	4.04	4.04	4.61	0.42	0.66	5.27	5.42
$H_3N\cdots BF_3$	1.472	1.92	1.85	2.75	1.85	2.52	5.17	6.17
$(CH_3)_3N\cdots BF_3$	0.61	0.74	0.96	2.57	2.05	2.81	5.24	6.11
$H_3N\cdots BH_3$	1.472	1.92	1.87	2.71	0.79	1.75	4.52	5.57
$(CH_3)_3N\cdots BH_3$	0.61	0.74	0.95	2.39	0.84	1.83	4.30	5.21
$H_3N\cdots B(CH_3)_3$	1.472	1.92	1.88	2.63	0.34	1.22	3.92	4.80
$(CH_3)_3N\cdots B(CH_3)_3$	0.61	0.74	1.04	2.28	0.39	1.28	3.65	4.60

[a] See text for discussion of symbols. [b] References to experimental dipole moments are given in Table 2.

TABLE 5: Computed Induced Dipole Moments (D) Using the BLW-ED Approach

species	$\Delta\mu_{dist}$(B)	$\Delta\mu_{dist}$(A)	$\Delta\mu_{pol}$(B)	$\Delta\mu_{pol}$(A)	$\Delta\mu_{CT}$(AB)	$\Delta\mu_{ind}$(theor)[a]	$\Delta\mu_{ind}$(expt.)[b]
$N_2\cdots SO_3$	0.0	0.0	0.28	0.11	0.05	0.44	0.46
$HCN\cdots SO_3$	0.0	0.22	0.58	0.33	0.22	1.35	1.43
$CH_3CN\cdots SO_3$	0.0	0.30	0.80	0.41	0.32	1.83	2.15
$H_3N\cdots SO_3$	−0.13	1.09	0.89	1.05	2.08	4.98	4.73
$(CH_3)_3N\cdots SO_3$	0.20	1.35	1.89	1.32	2.37	6.13	6.50
$HCN\cdots BF_3$	0.0	0.31	0.40	0.19	0.11	1.01	1.15
$CH_3CN\cdots BF_3$	0.0	0.42	0.57	0.24	0.15	1.38	*c*
$H_3N\cdots BF_3$	−0.07	1.85	0.90	0.67	1.00	4.35	4.43
$(CH_3)_3N\cdots BF_3$	0.22	2.05	1.61	0.76	0.87	5.51	5.40
$H_3N\cdots BH_3$	0.05	0.79	0.84	0.96	1.05	3.69	3.75
$(CH_3)_3N\cdots BH_3$	0.21	0.84	1.44	0.99	0.91	4.39	4.23
$H_3N\cdots B(CH_3)_3$	−0.04	0.34	0.75	0.88	0.88	2.81	*c*
$(CH_3)_3N\cdots B(CH_3)_3$	0.30	0.39	1.24	0.89	0.95	3.77	3.95

[a] Total of all calculated contributions to $\Delta\mu_{ind}$. [b] Calculated by subtraction of the dipole moment of the free base from the total complex dipole moment. [c] Not determined experimentally.

μ_{BLW}(AB) are also reported, as are those obtained from a full optimization at the Hartree-Fock (HF) level. For the free base, the calculated moments at the equilibrium geometry $\mu^0_{eq}(X)$ are also included and are compared with the experimental values μ(B). The dipole moments of the free Lewis acids are zero by symmetry and are not included. For the bases, the dipole moments calculated at the HF/6-31G(d) level of theory/basis set are seen to be systematically somewhat high, but again, because our concern is not in the absolute values of the dipole contributions but rather in the relative contributions to the induced moment, these discrepancies are not problematic. Table 5 gives the differences $\Delta\mu_{dist} = \mu^0(X) - \mu^0_{eq}(X)$, $\Delta\mu_{pol} = \mu_{BLW}(X) - \mu^0(X)$, and $\Delta\mu_{CT} = \mu_{HF}(AB) - \mu_{BLW}(AB)$ as well as the total induced moments determined both theoretically and experimentally. The observed and calculated induced moments are seen to agree to within a few tenths of a Debye.

Bond Moments. Calculations were also carried out with the intent of evaluating the bond moment approximation for SO_3, BF_3, and BH_3. Thus, dipole moments were calculated for each of these species at a series of pyramidally distorted structures. All calculations were done using Gaussian 98[40] with a 6-31G(2df) basis set at the MP2 level of theory. The calculated bond lengths at the planar configuration were 1.4353, 1.3091, and 1.1929 Å for SO_3, BF_3, and BH_3, respectively. These results compare favorably with the experimental values of 1.4198(2),[41] 1.3102(12),[42] and 1.190 01(1) Å,[43] indicating the suitability of the chosen basis set and level of theory.

The calculated dipole moments are plotted in Figure 2a against $\cos(\pi - \alpha)$, where α is the obtuse angle between the S−O, B−F, or B−H bonds and the C_3 axis of the molecule. In all cases, a near-linear relationship is observed across the full range of relevant angles, from which values of the S−O, B−F, and B−H bond moments can be determined. The values obtained are 2.32 D for the S−O bonds in SO_3, 2.45 D for the B−F bonds in BF_3, and 0.97 D for the B−H bonds in BH_3. The B−F bond moment of 2.45 D is in essentially exact agreement with that calculated from the 8° distorted structure given by Jurgens and Almlöf.[44] The 2.32 D value for SO_3 is somewhat less than the 3.0 D value we have used previously[16k,33] but is probably more reliable.

Induced Dipole Moments as a Function of Dative Bond Length. Finally, calculations of the full dipole moment function $\mu(R)$ were carried out for $H_3N{-}SO_3$ and $HCN{-}SO_3$ using Gaussian 98.[40] For $H_3N{-}SO_3$, both the 6-31G(2df) and aug-cc-pVTZ basis sets were used at the MP2 level. The choice of level of theory and basis set was made by carrying out geometry optimizations at a number of levels of theory employing several basis sets. Optimization using the 6-31G(2df) basis set yielded the best agreement with the experimentally determined moment while overestimating the N−S bond distance by about 0.07 Å. Optimizing with the larger aug-cc-pVTZ basis set gave better agreement with the experimental bond distance (to within ∼0.05 Å) but overestimated the dipole moment by 4%. To calculate $\mu(R)$, the N−S bond distance was fixed and partial optimizations were carried out at 0.05 Å intervals to obtain the molecular dipole moment. The induced moment at each N−S distance was obtained by subtraction of the NH_3 moment calculated at the corresponding level of theory/basis set. The results are plotted for both basis sets as the smooth curves in Figure 3a.

For $HCN{-}SO_3$, a similar procedure was carried out in order to select the appropriate level of theory and basis set. Calculations of $\mu(R)$ were carried out at both the HF and MP2 levels,

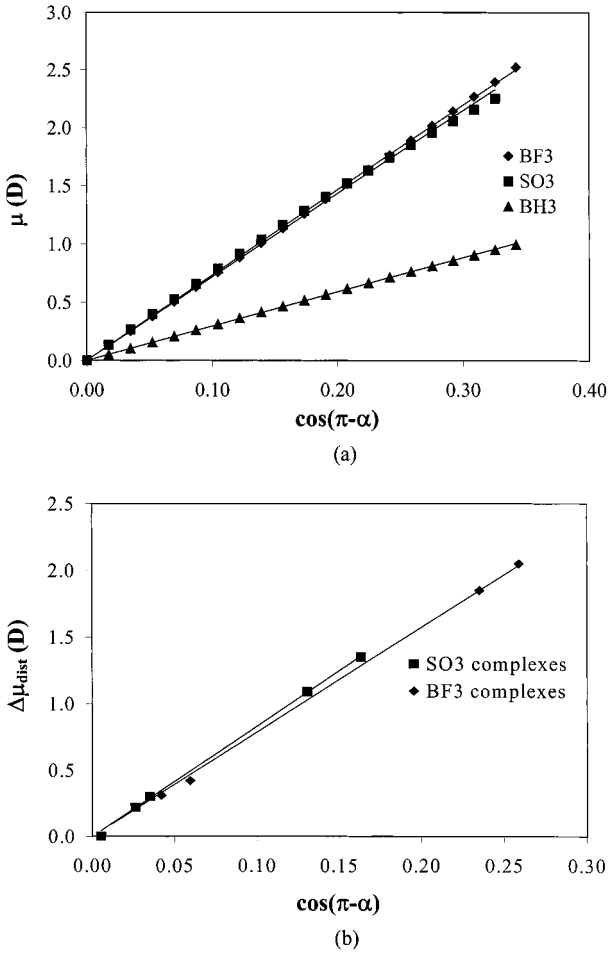

Figure 2. (a) Calculated dipole moments for SO_3, BF_3, and BH_3 vs $\cos(\pi - \alpha)$, where α is the obtuse angle formed from the S−O, B−F, or B−H bonds and the C_3 axis of the molecule. (b) $\Delta\mu_{dist}$(A) from BLW calculations vs $\cos(\pi - \alpha)$.

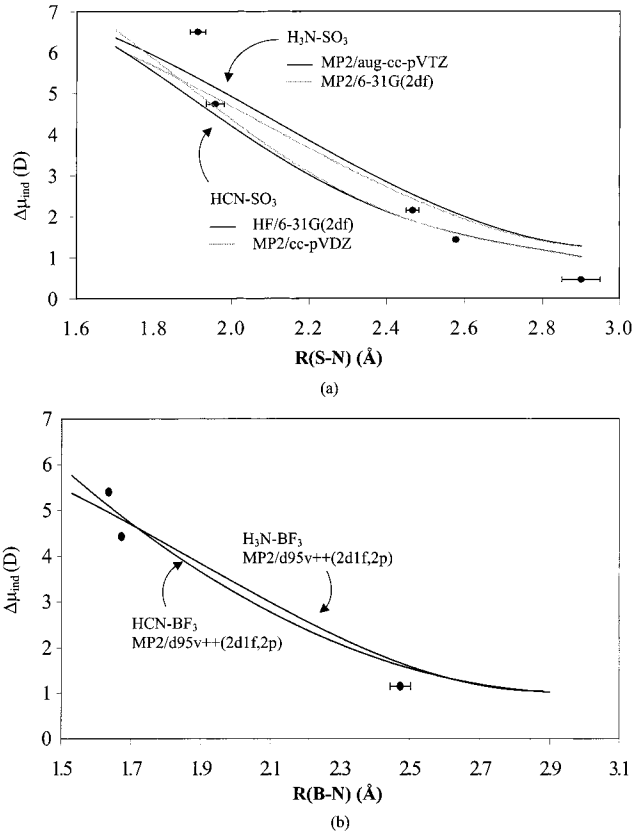

Figure 3. (a) Induced dipole moment as a function of S−O bond length for complexes of SO_3. The smooth curves are calculated, and the discrete points are experimental data from Table 2. The bond length for N_2−SO_3 is estimated from van der Waals radii and is shown with an error bar of ±0.05 Å (b) Induced dipole moment as a function of B−F bond length for complexes of BF_3. The smooth curves were generated from calculation of ref 18c, and the experimental data are from Table 2.

employing the 6-31G(2df) and cc-pVDZ basis sets, respectively. The N−S bond distance at the HF/6-31G(2df) level of theory/basis set was in closer agreement with the experimental value, whereas the dipole moment was 0.12 D too large. At the MP2/cc-pVDZ level, the dipole moment was almost in exact agreement with that determined experimentally; however, the N−S distance was overestimated by 0.20 Å. Again, the dipole moment was calculated with the N−S bond distance constrained at 0.05 Å intervals, and the induced moments were calculated by subtracting out the dipole moment of HCN obtained at the corresponding level of theory/basis set. The results are also plotted in Figure 3a.

Discussion

Experimental Results and BLW Decomposition. The set of complexes listed in Table 2 spans a wide range of dative bond distances and represents the full range from weak intermolecular interactions to genuine chemical bonds. N_2−SO_3, for example, is a van der Waals complex, whereas $(CH_3)_3N$−BF_3 and $(CH_3)_3N$−SO_3 are stable chemical species. Moreover, as we have noted previously[1,2,32,39] and as is seen again in Table 3, the bond angle at the acceptor atom for these systems correlates well with the donor−acceptor bond distance: Longer interaction distances are associated with a negligible distortion of the planar acid, whereas the shortest bond lengths are accompanied by near-tetrahedral geometries at the acceptor site. The systems may thus be regarded as points along the progression from van der Waals to chemical bonding. The induced moments are more useful than the dipole moments themselves for indicating changes in charge distribution throughout this progression, because they facilitate a comparison between systems containing bases with different values of μ(B). Note that zero-point averaging is not a significant issue for the purposes of comparison between these complexes, because it contributes only a small amount to the total induced dipole moments. For example, in HCN−SO_3, the projective reduction of μ_{HCN} along the symmetry axis of the complex, $\mu_{HCN}(1 - \cos\gamma)$, is just 0.03 D. Similar numbers are obtained for the other systems studied.

The most striking feature of the data is the sharp rise in the induced dipole moment as the length of the dative bond decreases. For example, in the series of SO_3 complexes with N_2, HCN, CH_3CN, H_3N, and $(CH_3)_3N$, the induced moments rise from 0.46 to 6.499 D as the N−S distance decreases from 2.9 to 1.912 Å. Likewise, in the BF_3 series, the observed values of $\Delta\mu_{ind}$ vary from 1.150 to 5.404 D as R(BN) decreases from 2.473 to 1.636 Å. These observations are consistent with the notion that a shorter bond distance is accompanied by more polarization, more charge transfer, and a larger component of the S−O and B−F bond moments along the symmetry axis of the complex.

The BLW results presented in Tables 4 and 5 provide an approximate decomposition of the observed moments into these constituent parts. As is shown in Table 5, the distortion of the base in all cases contributes little to the overall induced moment,

whereas the distortion of the acid contributes significantly. Moreover, it is evident that for the same base the contribution from the distortion of the acid is larger for the BF_3 complexes than for the SO_3 complexes, in accordance with the greater tendency toward a tetrahedral configuration at the boron (cf. Table 3). Indeed, plots of $\Delta\mu_{dist}$(A) from Table 5 vs $\cos(\pi - \alpha)$, shown in Figure 2b, resemble those of Figure 2a, maintaining a constant slope over the entire range of angles concerned. This indicates that $\Delta\mu_{dist}$(A) is reasonably regarded as arising from the reorientation of the polar S−O or B−F bonds in the acid. The bond moments obtained are 2.77 and 2.62 D for the S−O and B−F bonds in SO_3 and BF_3, respectively, which are similar to, though slightly larger than, the 2.32 and 2.45 D values reported above. The values derived from Figure 2a, however, are more reliable, because the level of theory and basis set were chosen to yield the closest agreement with the experimentally determined bond distances.

As is discussed in the Theoretical Background section, polarization is separated from charge-transfer effects in the BLW-ED approach by the construction of an "intermediate" wave function (eq 5), where the electron density of the respective fragments remains localized but is allowed to distort in response to the electric field of the nearby fragment. Table 5 demonstrates that the polarization component contributes significantly to the total induced moment for both the acid and base portions of the complex. For the acid, the polarization component increases as the length of the donor−acceptor bond decreases. This is a reasonable result, because a shortening of the dative bond is accompanied by an increasing angular distortion and therefore by a larger component of the B−F, B−H, or S−O bond polarizabilities along the primary axis of the complex. It is also consistent with the distance dependence of multipole-induced dipole interactions.[45] The polarization component of the basic portion is not necessarily subject to the same type of correlation with the structure because the bases have differing polarizabilities. However, for the bases represented in Table 5, a similar trend is indeed observed.

Finally, in Table 5, the charge-transfer component of the induced moment reveals the contribution arising from the physical transfer of electron density from the donor to the acceptor portion of the adduct. This is indicated by the difference between the dipole moment of the intermediate localized diabatic state and that obtained utilizing the final HF wave function. For the SO_3 complexes, the charge-transfer component of $\Delta\mu_{ind}$ clearly increases with decreasing bond length throughout the series. This, too, is a sensible result. For the BF_3 series, the trend is similar except that the charge-transfer component increases up to 1.0 D for $H_3N{-}BF_3$ and apparently then decreases to 0.87 D for the $(CH_3)_3N$ adduct. This ordering is preserved for the NH_3 and $(CH_3)_3N$ complexes of BH_3. For the two adducts of $(CH_3)_3B$, $\Delta\mu_{CT}$ increases slightly from NH_3 to $(CH_3)_3N$, but the calculated bond distance also *rises* from 1.739 Å in $NH_3{-}B(CH_3)_3$ to 1.825 Å in $(CH_3)_3N{-}B(CH_3)_3$. Thus, unlike the complexes of SO_3, the calculations indicate that for the H_3N and $(CH_3)_3N$ complexes of all three boron acids studied the shorter bond length is associated with the smaller value of $\Delta\mu_{CT}$. Such a reversal seems, at first, anomalous in light of the greater basicity of $(CH_3)_3N$ relative to that of NH_3. However, the calculated differences in $\Delta\mu_{CT}$ are small and may not be computationally significant. Moreover, even if real, whether they result from true differences in charge transfer or from differences in charge distribution within the resulting complexes cannot be inferred from the induced moments alone.

TABLE 6: Charge Transfer in Lewis Acid−Base Adducts

	charge transferred		
base···acid	Mulliken	NPA	hyperfine structure
$N_2{\cdots}SO_3$	0.0062	0.0019	
$HCN{\cdots}SO_3$	0.027	0.010	0.13[a]
$CH_3CN{\cdots}SO_3$	0.036	0.015	0.16[a]
$H_3N{\cdots}SO_3$	0.27	0.21	0.36[b]
$(CH_3)_3N{\cdots}SO_3$	0.31	0.26	0.58[c]
$HCN{\cdots}BF_3$	0.015	0.0078	
$CH_3CN{\cdots}BF_3$	0.020	0.012	
$H_3N{\cdots}BF_3$	0.22	0.12	0.26[d]
$(CH_3)_3N{\cdots}BF_3$	0.20	0.12	0.41[e]
$H_3N{\cdots}BH_3$	0.26	0.13	
$(CH_3)_3N{\cdots}BH_3$	0.26	0.13	0.41[f]
$H_3N{\cdots}B(CH_3)_3$	0.18	0.11	
$(CH_3)_3N{\cdots}B(CH_3)_3$	0.14	0.12	0.40[e]

[a] Reference 32. [b] Reference 33. [c] Reference 16k. [d] Calculated from the data of ref 46. [e] Reference 47. [f] Calculated from the data of ref 48.

Charge Transfer. To provide a more quantitative comparison of the degree of charge transfer in the systems considered here, Mulliken and natural population analyses (NPA) were carried out for both the BLW and HF wave functions. Although charges assigned in this fashion are inherently arbitrary, the approach remains useful for a comparison between similar complexes. Because of the localized nature of the BLW wave function, the charge-transfer contribution to the total density is identically zero; thus, the magnitude of the charge transfer is equal to the excess charge on the acid portion of the complex at the HF level. Table 6 summarizes the results.

For the complexes of SO_3, both the Mulliken and NPA populations indicate an increase in charge transfer with a decrease in bond length. For the complexes of BF_3, on the other hand, the Mulliken analysis indicates a rise in charge transfer up to the NH_3 complex, followed by a small decrease for the $(CH_3)_3N$ adduct. However, although this apparent reversal is reminiscent of that noted above for $\Delta\mu_{CT}$, it is not reproduced by the NPA analysis, which indicates essentially the same degree of charge transfer in $H_3N{-}BF_3$ and $(CH_3)_3N{-}BF_3$. Similar results are obtained for $H_3N{-}B(CH_3)_3$ and $(CH_3)_3N{-}B(CH_3)_3$, but $H_3N{-}BH_3$ and $(CH_3)_3N{-}BH_3$ appear to have the same degree of charge-transfer regardless of the method of population analysis used.

The increase in charge transfer observed across the SO_3 series is consistent with the increasing basicity of the electron-pair donors that accompanies the decreasing bond length. On the other hand, although $HCN{-}BF_3$, $CH_3CN{-}BF_3$, and $H_3N{-}BF_3$ behave in a similar orderly fashion, the results for the H_3N and $(CH_3)_3N$ complexes of the boron acids are ambiguous. The Mulliken population analysis has been widely criticized, especially for its basis set dependence,[49] and the counterintuitive results obtained for these bases should be viewed with caution. Indeed, in light of the NPA analyses, it seems more likely that the differences in charge transfer between the H_3N and $(CH_3)_3N$ adducts of these boron acids are too small to discern.

To provide a pictorial representation of the changes in the charge density accompanying both charge transfer and polarization, electron density difference plots were generated for $HCN{-}SO_3$, $(CH_3)_3N{-}SO_3$, and $(CH_3)_3N{-}BF_3$ and are shown in Figure 4. From the figure, it is clear that there is almost no charge transfer in the $HCN{-}SO_3$ complex, whereas polarization tends to move the charge density outward toward the SO_3 oxygens on the acid portion and away from the SO_3 on the HCN. For the two $(CH_3)_3N$ complexes, the effect of polarization is to distort the charge density away from the nitrogen atomic center

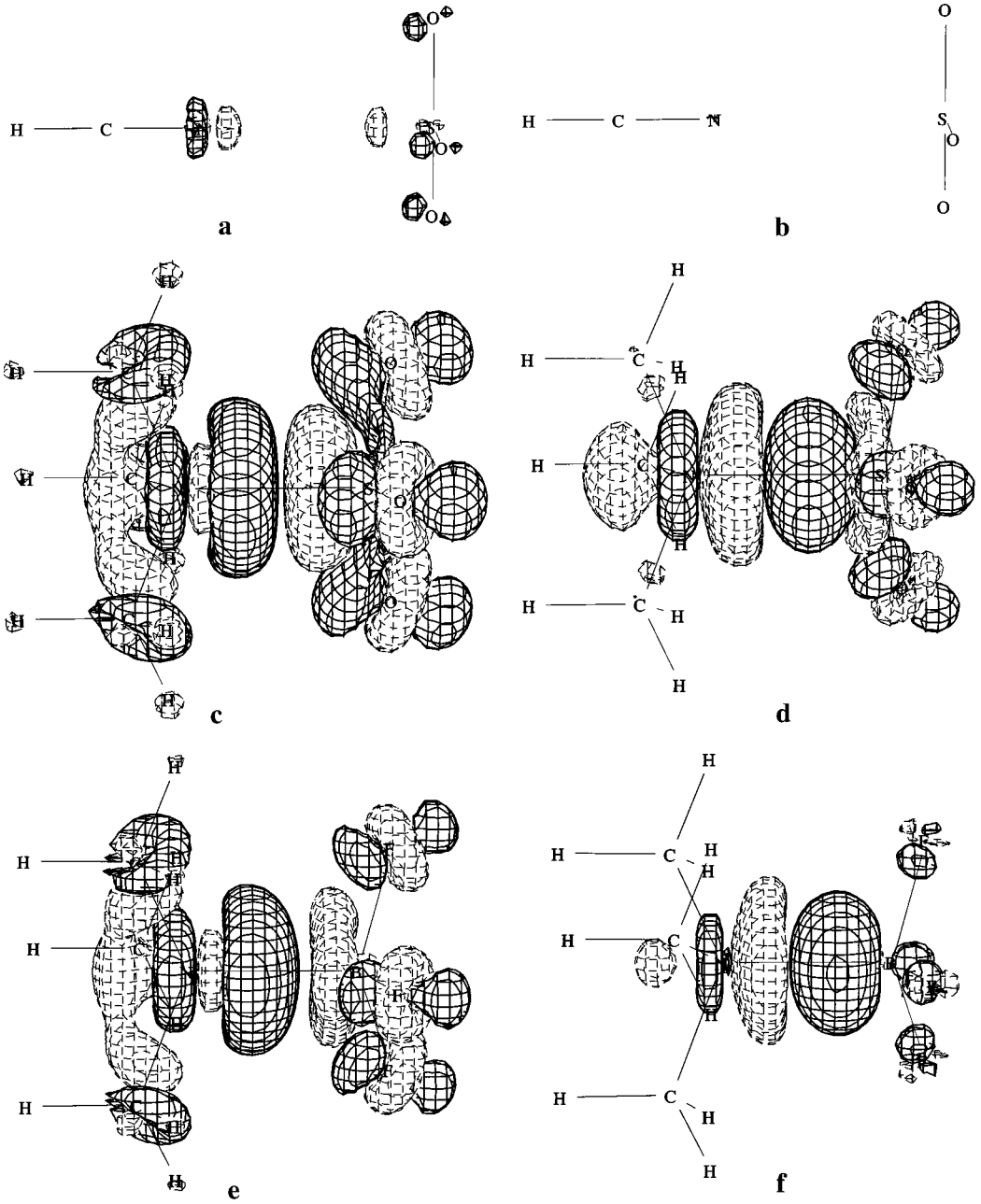

Figure 4. Electron density difference plots for (a) $HCN-SO_3$, polarization; (b) $HCN-SO_3$, charge transfer; (c) $(CH_3)_3N-SO_3$, polarization; (d) $(CH_3)_3N-SO_3$, charge transfer; (e) $(CH_3)_3N-BF_3$, polarization; and (f) $(CH_3)_3N-BF_3$, charge transfer. Heavy lines indicate an increase in the charge density. Dashed lines indicate a decrease in the charge density. The contour level is 0.005 e/au^3.

into the bonding region while at the same time increasing the density in the region of the carbon atoms. The polarization of SO_3 and BF_3 can be seen as arising largely from orbital rehybridization on the oxygens or fluorines. The effect of charge transfer is a further migration of charge density from the region near the N position to that of the Lewis acid, with a concomitant increase in charge density on the oxygens or fluorines along the S−O or B−F bond axes, respectively. These results are similar to previous calculations of the charge density of NH_3-SO_3.[7,38] The significant involvement of charge density on the methyl groups of trimethylamine carbons is also consistent with experimental evidence from (e, 2e) spectroscopy, which indicates significant delocalization of the "lone pair" orbital on the carbons.[50]

It is also of interest to examine the question of charge transfer from an experimental standpoint. Estimates of charge transfer can be made from the analysis of nuclear quadrupole coupling constants,[27,51] with the standard approach being that first given by Townes and Dailey.[52] A number of results derived from the analysis of the ^{14}N coupling constants are available for the complexes examined in this work and are also given in Table 6. In obtaining these values, the one-electron wave function for the dative bond is assumed to have the simple form $\Psi = \alpha\phi_D + \beta\phi_A$, where ϕ_D and ϕ_A are the donor and acceptor orbitals, respectively. A value of $2\beta^2$, interpreted as the "charge transfer", is derived from quadrupole coupling constants subject to the usual assumptions of the Townes and Dailey method and to neglect of overlap between ϕ_D and ϕ_A. As is applied to donor−acceptor complexes, this approach also assumes that any change in the quadrupole coupling constant from its free monomer value can be attributed to the transfer of charge from the basic portion of the adduct to the acid. The values obtained are thus very approximate and probably represent upper limits to the true electron transfer.

TABLE 7: Comparison of Calculated and Experimental Dipole Moments

complex	*n*	μ_{EXP} (D)	μ_{calc} (D)[a]	% difference[b]
$HCN-SO_3$	0.13	4.4172(31)	4.82	−9
CH_3CN-SO_3	0.16	6.065(18)	6.06	0
H_3N-SO_3	0.36	6.204(11)	5.79	7
$(CH_3)_3N-SO_3$	0.58	7.1110(69)	7.17	−1
H_3N-BF_3	0.26[c]	5.9027(93)	5.30	10
$(CH_3)_3N-BF_3$	0.41	6.0157(76)	5.92	2
$(CH_3)_3N-BH_3$	0.40[d]	4.84(10)[d]	4.53	6

[a] Calculated from eq 9. [b] $100(\mu_{EXP} - \mu_{calc})/\mu_{EXP}$. [c] Calculated from ref 46. [d] Reference 48.

The experimentally derived values in Table 6 may be compared with the results of the Mulliken and NPA population analyses. Such a comparison is complicated, of course, by the fact that neither approach yields the "correct" electron-transfer value. Indeed, superficially, it appears from the table that the degree of charge transfer obtained from a Townes and Dailey analysis is overestimated,[53] but in light of the substantially different nature of these estimates, it is unclear how well the experimental values are expected to agree with those derived from population analyses. Nonetheless, despite these complications, the trend toward increasing electron transfer at shorter bond distances is reproduced in the SO_3 series. In the case of the boron-containing adducts, there is insufficient experimental data to establish a trend. However, it is interesting to note that the charge transfer derived from hyperfine structure appears significantly larger in $(CH_3)_3N-BF_3$ than in H_3N-BF_3, in contrast with the theoretical results described above.

Implications for a Simplistic Chemical Viewpoint. In two previous studies, we presented a simple model that appeared to predict the observed dipole moments of H_3N-SO_3[33] and $(CH_3)_3N-SO_3$[16k] to within only a few percent. The model is based on elementary ideas of bond moments and charge transfer and takes the following form:

$$\mu = \mu(\mathrm{B}) + 3\mu_{MX}\sin(\alpha - 90) + neR \qquad (9)$$

Here, μ(B) is the dipole moment of the free base, μ_{MX} is the bond moment of an S−O or B−F bond (obtained from Figure 2a), $n \equiv 2\beta^2$, and R is the N−S or N−B bond distance. According to eq 9, the dipole moment of the complex arises mainly from that of the base, that of the distorted acid, and that resulting from the transfer of n electrons across the distance of the donor−acceptor bond.

Although eq 9 appeared to be successful in our previous work, we noted that the *neR* term is a grossly oversimplified expression of the charge-transfer component and that mutual polarization of the interacting moieties is neglected. Moreover, the validity of the bond moment approximation, inherent in the second term of eq 9, is not guaranteed. Thus, it is of interest to ascertain whether similar results can be achieved for other systems as well or whether the apparent success for H_3N-SO_3 and $(CH_3)_3N-SO_3$ is fortuitous. Table 7 presents the results of eq 9 for the complexes investigated in this work for which all of the necessary experimental data are available. The results for H_3N-SO_3 and $(CH_3)_3N-SO_3$ differ slightly from those reported in our previous work because of the use of the improved S−O bond moment determined above. Remarkably, all of the observed dipole moments are predicted to within about 10%.

Some insight into the apparent success of this model can be gained from the computational results presented above. From Figure 2a, it is clear that the B−F and S−O bond moments are well defined, and thus the second term in eq 9 reasonably corresponds to the $\Delta\mu_{dist}$ term calculated in the BLW method. In addition, values of $\Delta\mu_{dist}$(B) given in Table 5 are small, so that the neglect of structural distortion of the base, implied by eq 9, also appears valid. However, it is clear from the BLW results that electronic polarization of both the acid and base gives rise to substantial contributions to the dipole moment of the complex. Thus, the neglect of polarization is a significant omission from the simple model, and it seems likely that the *neR* term overestimates the charge-transfer component by an amount that approximately compensates for this neglect. Indeed, values of *neR* calculated from hyperfine structure run some 1.6−7.3 times larger than the corresponding $\Delta\mu_{CT}$ values obtained from the BLW method, with the larger ratios occurring for the more weakly bound systems. Such a situation is consistent with the notion that the Townes and Dailey analysis provides an upper limit to the charge transfer and that the polarization contribution to *eQq* is most significant when charge transfer is not the major contributor. Differences in charge distribution may also play a significant role. In any case, a scenario involving the cancellation of terms is consistent with the observation that the calculated dipole moments are neither systematically high nor systematically low. In addition, the percent accuracy quoted in Table 7 may artificially glorify the quality of the calculation, because the dipole moments themselves are large and a substantial residual is still a relatively small percentage of the total moment.

The success of this model demonstrates the arbitrariness of partitioning charge-transfer and polarization effects in systems where both contribute significantly to the bonding interaction. In the Townes and Dailey model, it is common to summarize all of the changes in electron density at a particular nucleus into a single parameter, which is referred to as "charge transfer". However, this parameter describes not only real charge transfer but charge migration due to distortion of the electron density produced by the local electric field. Thus, the terms "charge transfer" and polarization lose their clarity, and the distinction between the two coactive effects becomes uncertain. The BLW-ED approach allows for a solution to this problem by the construction of the intermediate diabatic state, an unphysical state where the electron density is forced to remain localized but is allowed to distort in the presence of the nearby electric field. Physical charge transfer is thus partitioned from polarization and obtained only in the final step, where the restriction of localization is relaxed and the charge is allowed to delocalize and become associated with molecular orbitals on the nearby fragment. This offers a *definition* of charge transfer, one that effectively separates out polarization, which in the end may or may not turn out to be the most reliable method. For the purposes here, the approach has provided considerable insight into the electronic changes that accompany the formation of the dative bond and contribute to the measured dipole moments in these systems.

Radial Dependence of the Induced Moment. A final question arising from the observed induced dipole moments involves not their magnitude, per se, but rather their variation with bond length. As is noted in the Introduction, the sensitivity of partially bonded systems to a local environment appears to be closely related to an increasing dipole moment function at shorter dative bond distances. The experimental determination of $\mu(R)$, however, is in general nontrivial, and indeed, whereas large structure changes upon crystallization are well documented experimentally, support for a "dipolar enhancement" mechanism is largely theoretical.[5,7−10] We have noted, however, that $\Delta\mu_{ind}$ increases as the bond length decreases across a series of

complexes with a common base. Therefore, a natural question concerns the possibility that the dipole moments of a series contain information about the radial dependence of $\Delta\mu_{ind}$. Such an idea, while not rigorously justifiable, would be akin to the widely used structure-correlation method for determining reaction paths from crystallographic data.[4]

The results shown in Figure 3a address this question for complexes of SO_3. Similar calculations of $\Delta\mu_{ind}(R)$ have been carried out previously for $HCN-BF_3$[18c] and H_3N-BF_3,[16i,18c] and the results are reproduced in Figure 3b. For both sets of systems, the theoretical curves for the HCN and NH_3 complexes are seen to be similar, though exact agreement is neither observed nor expected. Equally important is that for both sets of systems, although the number of experimental points is small, a rough correspondence between the experimental values and the theoretical results is suggested. In other words, values of $\Delta\mu_{ind}$ for a set of different complexes of SO_3 at their zero-point geometries roughly indicate the value to be found for $HCN-SO_3$ and H_3N-SO_3 at bond lengths far from equilibrium. A similar situation is suggested for complexes of BF_3, though fewer experimental points are available.

Although the above result is not rigorously guaranteed, it is reasonable in the following sense: In a previous paper, we used a series of BF_3 complexes with nitrogen donors to test the validity of the structure-correlation method for determining reaction paths.[18c] We found that the relationship between bond length, *R*, and the NBF bond angle, α, across a series of complexes was in reasonable agreement with that calculated theoretically for a single complex across the full range of relevant B−N distances. Thus, the evolution of the molecular structure is similar among members of the series as bond formation proceeds. This is a chemically sensible idea and is the essence of the structure-correlation method. If one subscribes to this general viewpoint, then it is a relatively small extrapolation to suppose that changes in charge distribution that occur upon formation of the dative bond similarly follow a common, generalized pathway. Changes arising from electrostatic polarization will, of course, depend on the polarizabilities and multipole moments of the particular base and do not necessarily vary smoothly across a series. However, for the complexes investigated here, such effects apparently do not obscure the correlation. Indeed, in general, such a method might prove useful for estimating dipole moment functions for systems of this kind. In effect, the large dynamic range associated with the bonding across a series of related complexes allows the radial dependence of the induced moment to be probed without the usual need for vibrational excitation along the bond coordinate.

Conclusions

Dipole moments have been measured for a series of Lewis acid−base complexes in the gas phase. The results have been analyzed, together with literature values for a number of closely related systems, to elucidate the changes in polarity that occur across the full range between van der Waals interactions and chemical bonds. The induced dipole moments for the adducts studied are large and increase sharply as the length of the donor−acceptor bond decreases. Moreover, decomposition of the dipole moments using a block-localized wave function scheme indicates that polarization of the acid and base, charge transfer, and geometrical distortion of the acid all contribute significantly to the overall dipole moment of the complexes. The geometrical distortion of the base, on the other hand, contributes negligibly. The contributions to the total dipole moment arising from polarization, charge transfer, and distortion each individually exhibit a general increase as the donor−acceptor bond length decreases, though a few small anomalies may exist.

Charge transfer, as determined theoretically by population analyses and experimentally from nuclear hyperfine structure, also generally increases for the systems studied as the donor−acceptor bond shortens. A possible exception involves the H_3N and $(CH_3)_3N$ adducts of BF_3, BH_3, and $(CH_3)_3B$. A comparison between experimental and theoretical values is difficult, because the two measures are defined in substantially different ways. Nonetheless, the experimentally derived estimates are systematically larger than those obtained from population analysis. A simple model involving bond moments and experimental charge-transfer values appears to predict the measured dipole moments reasonably well, but the success likely arises from an accidental cancellation involving an overestimate of charge transfer and neglect of polarization.

Finally, calculations of the induced dipole moment as a function of bond length have been presented for several of the systems studied. The results are compared with experimental values for a series of complexes of different dative bond lengths. We find that for the systems investigated here the induced moments of the *series* roughly approximate the induced dipole moment *function* for individual members of the series. Thus, a group of complexes taken as a whole contains approximate information about the radial dependence of $\Delta\mu_{ind}$, much like crystallographic and gas-phase structure correlations contain information about reaction pathways.

Acknowledgment. This work was supported by the National Science Foundation (CHE-9730844) and the donors of the Petroleum Research Fund, administered by the American Chemical Society. A.R. was supported by an NSF REU Grant at the University of Minnesota, and support for the computational work was obtained from the Minnesota Supercomputer Institute. We are especially grateful to Prof. Jiali Gao for valuable input and to Dr. Deborah Hankinson for providing us with the numerical data used to regenerate Figure 3b.

Supporting Information Available: Tables of Stark shifted transition frequencies and residuals from least-squares fits. This material is available free of charge via the Internet at http://pubs.acs.org.

References and Notes

(1) Leopold, K. R. In *Advances in Molecular Structure Research*; Hargittai, M., Hargittai, I., Eds.; JAI Press: Greenwich, CT, 1996; Vol. 2, p 103 and references therein.

(2) Leopold, K. R.; Canagaratna, M.; Phillips, J. A. *Acc. Chem. Res.* **1997**, *30*, 57 and references therein.

(3) Bent, H. A. *Chem. Rev.* **1968**, *68*, 587 and references therein.

(4) (a) Bürgi, H.-B.; Dunitz, J. D. *Acc. Chem. Res.* **1983**, *16*, 153 and references therein. (b) *Structure Correlation*; Bürgi, H.-B., Dunitz, J. D., Eds.; VCH Publishers: Weinheim, Germany, 1994; and references therein.

(5) Oh, J. J.; LaBarge, M. S.; Matos, J.; Kampf, J. W.; Hillig, K. W., II; Kuczkowski, R. L. *J. Am. Chem. Soc.* **1991**, *113*, 4732.

(6) (a) Forgács, G.; Kolonits, M.; Hargittai, I. *Struct. Chem.* **1990**, *1*, 245. (b) Shen, Q.; Hilderbrandt, R. L. *J. Mol. Struct.* **1980**, *64*, 257.

(7) Wong, M. W.; Wiberg, K. B.; Frisch, M. J. *J. Am. Chem. Soc.* **1992**, *114*, 523.

(8) Bühl, M.; Steinke, T.; Schleyer, P. v. R.; Boese, R. *Angew. Chem., Int. Ed. Engl.* **1991**, *30*, 1160.

(9) Jiao, H.; Schleyer, P. v. R. *J. Am. Chem. Soc.* **1994**, *116*, 7429.

(10) Cioslowski, J.; Martinov, M. *J. Chem. Phys.* **1995**, *103*, 4967.

(11) Lewis, G. N. *Valence and the Structure of Atoms and Molecules*; The Chemical Catalog Co., Inc.: New York, 1923.

(12) For example, see: (a) Hargittai, M.; Hargittai, I. *The Molecular Geometries of Coordination Compounds in the Vapor Phase*; Elsevier: Amsterdam, The Netherlands, 1977. (b) *Spectroscopy and Structure of Molecular Complexes*; Yarwood, J., Ed.; Plenum: London, 1973. (c)

Mulliken, R. S.; Person, W. B. *Molecular Complexes. A Lecture and Reprint Volume*; Wiley: New York, 1969. (d) Satchell, D. P. N.; Satchell, R. S. *Q. Rev., Chem. Soc.* **1971**, *25*, 171. (e) Hargittai, M.; Hargittai, I. *Phys. Chem. Miner.* **1987**, *14*, 413.

(13) (a) Mulliken, R. S. *J. Am. Chem. Soc.* **1952**, *74*, 811. (b) Mulliken, R. S. *J. Phys. Chem.* **1952**, *56*, 801.

(14) Gal, J.-F.; Maria, P. C. *Prog. Phys. Org. Chem.* **1990**, *117*, 159.

(15) For example, see: (a) Hargittai, M.; Hargittai, I. *J. Mol. Struct.* **1977**, *39*, 79. (b) Iijma, K.; Adachi, N.; Shibata, S. *Bull Chem. Soc. Jpn.* **1984**, *57*, 3269. (c) Anderson, G. A.; Forgaard, F. R.; Haaland, A. *Acta Chem. Scand.* **1972**, *26*, 1947. (d) Almond, M. J.; Jenkins, C. E.; Rice, D. A.; Hagen, K. *J. Organomet. Chem.* **1992**, *439*, 251.

(16) For example, see: (a) Odom, J. D.; Kalasinsky, V. F.; Durig, J. R. *Inorg. Chem.* **1975**, *11*, 2837. (b) Cassoux, P.; Kuczkowski, R. L.; Bryan, P. S.; Taylor, R. C. *Inorg. Chem.* **1975**, *14*, 126. (c) Cassoux, P.; Kuczkowski, R. L.; Serafini, A. *Inorg. Chem.* **1977**, *16*, 3005. (d) Stevens, J. F., Jr.; Bevan, J. W.; Curl, R. F., Jr.; Geanangel, R. A.; Hu, M. G. *J. Am. Chem. Soc.* **1977**, *99*, 1442. (e) Kuznesof, P. M.; Kuczkowski, R. L. *Inorg. Chem.* **1978**, *17*, 2308. (f) Thorne, L. R.; Suenram, R. D.; Lovas, F. J. *J. Chem. Phys.* **1983**, *78*, 167. (g) Oh, J. J.; Hillig, K. W., II; Kuczkowski, R. L. *J. Phys. Chem.* **1991**, *95*, 7211. (h) Warner, H. E.; Wang, Y.; Ward, C.; Gillies, C. W.; Interrante, L. *J. Phys. Chem.* **1994**, *98*, 12215. (i) Fujiang, D.; Fowler, P. W.; Legon, A. C. *J. Chem. Soc., Chem. Commun.* **1995**, 113. (j) Müller, J.; Ruschewitz, U.; Indris, O.; Hartwig, H.; Stahl, W. *J. Am. Chem. Soc.* **1999**, *121*, 4647. (k) Fiacco, D. L.; Toro, A.; Leopold, K. R. *Inorg. Chem.* **2000**, *39*, 37.

(17) For example, see: (a) Piocos, E. A.; Ault, B. S. *J. Phys. Chem.* **1992**, *96*, 7589. (b) Piocos, E. A.; Ault, B. S. *J. Phys. Chem.* **1993**, *97*, 3492. (c) Beattie, I. R.; Jones, P. J. *Angew. Chem., Int. Ed. Engl.* **1996**, *35*, 1527.

(18) For example, see: (a) Jonas, V.; Frenking, G.; Reetz, M. T. *J. Am. Chem. Soc.* **1994**, *116*, 8741. (b) Fradera, X.; Austen, M. A.; Bader, R. F. W. *J. Phys. Chem. A* **1999**, *103*, 304. (c) Hankinson, D. J.; Almlöf, J.; Leopold, K. R. *J. Phys. Chem.* **1996**, *100*, 6904. (d) Cabaleiro-Lago, E. M.; Ríos, M. A. *Chem. Phys. Lett.* **1998**, *294*, 272. (e) Iglesias, E.; Sordo, T. L.; Sordo, J. A. *Chem. Phys. Lett.* **1996**, *248*, 179. (f) Skancke, A.; Skancke, P. N. *J. Phys. Chem.* **1996**, *100*, 15079. (g) Ford, T. A.; Steele, D. *J. Phys. Chem.* **1996**, *100*, 19336. (h) Branchadell, V.; Sbai, A.; Oliva, A. *J. Phys. Chem.* **1995**, *99*, 6472. (i) Glendening, E. D.; Streitwieser, A. *J. Chem. Phys.* **1994**, *100*, 2900.

(19) (a) Laubengayer, A. W.; Sears, D. S. *J. Am. Chem. Soc.* **1945**, *67*, 164. (b) McClellan, A. L. *Tables of Experimental Dipole Moments*; Freeman: San Francisco, CA, 1963.

(20) Canagaratna, M.; Ott, M. E.; Leopold, K. R. *Chem. Phys. Lett.* **1997**, *281*, 63.

(21) Balle, T. J.; Flygare, W. H. *Rev. Sci. Instrum.* **1981**, *52*, 33.

(22) (a) Phillips, J. A.; Canagaratna, M.; Goodfriend, H.; Grushow, A.; Almlöf, J. *J. Am. Chem. Soc.* **1995**, *117*, 12549. (b) Phillips, J. Ph.D. Thesis, The University of Minnesota, Minneapolis, MN, 1996.

(23) Muenter, J. S. *J. Chem. Phys.* **1968**, *48*, 4544.

(24) Bowen, K. H.; Leopold, K. R.; Chance, K. V.; Klemperer, W. *J. Chem. Phys.* **1980**, *73*, 137.

(25) Coudert, L. H.; Lovas, F. J.; Suenram, R. D.; Hougen, J. T. *J. Chem. Phys.* **1987**, *87*, 6290.

(26) (a) Adams, R.; Brown, B. K. In *Organic Synthesis*, 2nd ed.; Gilman, H., Blatt, A. H., Eds.; Wiley: New York, 1941; Collect. Vol. No. 1, p 528. (b) Clippard, P. H. Ph.D. Thesis, The University of Michigan, Ann Arbor, MI, 1969.

(27) Gordy, W.; Cook, R. L. *Microwave Molecular Spectra*; Wiley: New York, 1984.

(28) Maki, A. G. *J. Phys. Chem. Ref. Data* **1974**, *3*, 221.

(29) Beers, Y.; Russell, T. W. *IEEE Trans. Instrum. Meas.* **1966**, *IM-15*, 380.

(30) Marshall, M. D.; Muenter, J. S. *J. Mol. Spectrosc.* **1981**, *85*, 322.

(31) Lide, D. R.; Mann, D. E. *J. Chem. Phys.* **1958**, *28*, 572.

(32) Burns, W. A.; Phillips, J. A.; Canagaratna, M.; Goodfriend, H.; Leopold, K. R. *J. Phys. Chem. A* **1999**, *103*, 7445.

(33) Canagaratna, M.; Phillips, J. A.; Goodfriend, H.; Leopold, K. R. *J. Am. Chem. Soc.* **1996**, *118*, 5290.

(34) Coppens, P.; Guru Row, T. N.; Leung, P.; Stevens, E. D.; Becker, P. J.; Yang, Y. W. *Acta Crystallogr.* **1979**, *A35*, 63.

(35) Bats, J. W.; Coppens, P.; Koetzle, T. F. *Acta Crystallogr.* **1977**, *B33*, 37.

(36) Reeve, S. W.; Burns, W. A.; Lovas, F. J.; Suenram, R. D.; Leopold, K. R. *J. Phys. Chem.* **1993**, *97*, 10630.

(37) Lide, D. R., Jr.; Taft, R. W., Jr.; Love, P. *J. Chem. Phys.* **1959**, *31*, 561.

(38) Mo, Y.; Gao, J.; Peyerimhoff, S. D. *J. Chem. Phys.* **2000**, *112*, 5530.

(39) Dvorak, M. A.; Ford, R. S.; Suenram, R. D.; Lovas, F. J.; Leopold, K. R. *J. Am. Chem. Soc.* **1992**, *114*, 108.

(40) Frisch, M. J.; Trucks, G. W.; Schlegel, H. B.; Scuseria, G. E.; Robb, M. A.; Cheeseman, J. R.; Zakrzewski, V. G.; Montgomery, J. A., Jr.; Stratmann, R. E.; Burant, J. C.; Dapprich, S.; Millam, J. M.; Daniels, A. D.; Kudin, K. N.; Strain, M. C.; Farkas, O.; Tomasi, J.; Barone, V.; Cossi, M.; Cammi, R.; Mennucci, B.; Pomelli, C.; Adamo, C.; Clifford, S.; Ochterski, J.; Petersson, G. A.; Ayala, P. Y.; Cui, Q.; Morokuma, K.; Malick, D. K.; Rabuck, A. D.; Raghavachari, K.; Foresman, J. B.; Cioslowski, J.; Ortiz, J. V.; Baboul, A. G.; Stefanov, B. B.; Liu, G.; Liashenko, A.; Piskorz, P.; Komaromi, I.; Gomperts, R.; Martin, R. L.; Fox, D. J.; Keith, T.; Al-Laham, M. A.; Peng, C. Y.; Nanayakkara, A.; Challacombe, M.; Gill, P. M. W.; Johnson, B.; Chen, W.; Wong, M. W.; Andres, J. L.; Gonzalez, C.; Head-Gordon, M.; Replogle, E. S.; Pople, J. A. *Gaussian 98*, Revision A.9; Gaussian, Inc.: Pittsburgh, PA, 1998.

(41) (a) Meyer, V.; Sutter, D. H.; Dreizler, H. *Z. Naturforsch., A*: *Phys. Sci.* **1991**, *46*, 710. (b) Kaldor, A.; Maki, A. G. *J. Mol. Spectrosc.* **1973**, *15*, 123.

(42) Brown, C. W.; Overend, J. *Can. J. Phys.* **1968**, *46*, 977.

(43) Kawaguchi, K. *J. Chem. Phys.* **1992**, *96*, 3411.

(44) Jurgens, R.; Almlöf, J. *Chem. Phys. Lett.* **1991**, *176*, 263.

(45) Curiously, the calculated values of $\Delta\mu_{pol}(A)$ given in Table 5 exhibit a strikingly linear dependence on $\cos(\alpha)$ for both the SO_3 and BF_3 series of adducts. Although a dependence on $\cos(\alpha)$ is certainly to be expected, the variability of dipole and higher order multiple moments of the bases across the series render this linearity interesting but of no obvious fundamental significance.

(46) Legon, A. C.; Warner, H. E. *J. Chem. Soc., Chem. Commun.* **1991**, 1397.

(47) Fiacco, D. L.; Hunt, S. W.; Leopold, K. R. *54th Symposium on Molecular Spectroscopy*; Columbus, OH, 1999; Abstract WF12.

(48) Kasten, W.; Dreizler, H.; Kuczkowski, R. L. *Z. Naturforsch* **1985**, *40A*, 1262.

(49) For example, see: Bachrach, S. M. In *Reviews in Computational Chemistry*; Lipkowitz, K. B., Boyd, D. B., Eds.; VCH: New York, 1994; Vol. 5.

(50) McMillan, K.; Coplan, M. A.; Moore, J. H.; Tossell, J. A. *J. Phys. Chem.* **1990**, *94*, 8648.

(51) Lucken, E. A. C. *Nuclear Quadrupole Coupling Constants*; Academic Press: London, 1969.

(52) Townes, C. H.; Dailey, B. P. *J. Chem. Phys.* **1949**, *17*, 782.

(53) It is interesting to note that the inclusion of even modest overlap integrals in the calculation of $2\beta^2$ significantly reduces the value obtained. Hunt, S. W.; Leopold, K. R. Manuscript in preparation.